Tristate Converters with Limited Duty Cycle

FELIX A. HIMMELSTOSS
Faculty of Electronic Engineering and Entrepreneurship,
University of Applied Sciences Technikum Wien,
Hoechstaedtplatz 6, 1200 Vienna,
AUSTRIA

Abstract: - Replacing the active switch of a DC/DC converter with a series connection of two active switches and a diode which is connected to the connection point of the two switches, changes the converter into a tristate one. The tristate concept changes the voltage transformation ratio of the original converter and influences the dynamics. Starting from a topology for limited duty cycles, four converters can be derived. There are two possibilities for the position of the second capacitor and so eight converter structures can be achieved. The position of the second capacitor influences the input current, the inrush, the stored energy, and the voltage stress of this component. When the input voltage has the other polarity, again eight converters can be designed. Changing all active electronic switches by current bidirectional ones (an electronic switch with an antiparallel diode) leads to bidirectional converters and increases the number of converters that are derived from the basic topology to thirty-two. The function of the four basic structures is explained, and the voltage transformation ratio calculated and graphically shown. The connections of the currents are explained. For one converter the large and the small signal models and two transfer functions are calculated, and simulation of the dynamics are shown.

Key-Words: - DC/DC converter, tristate, step-up, step-down, step-up-down, voltage transformation ratio

Received: February 16, 2023. Revised: November 25, 2023. Accepted: December 14, 2023. Published: December 31, 2023.

1 Introduction

The starting point of this review and study is the paper, [1], which describes converters with limited duty cycles. The basic topology is shown in Figure 1. In the original paper the symbolic switches SStr1 and SStr2 are current bidirectional switches, voltage bidirectional switches, diodes, or AC switches, or combinations of them. So one can construct DC/DC, DC/AC, AC/DC, and AC/AC converters. The second capacitor can be placed in parallel to the load or between the input and the output. In this paper, the tristate concept is applied to the converter concept according to Figure 1.

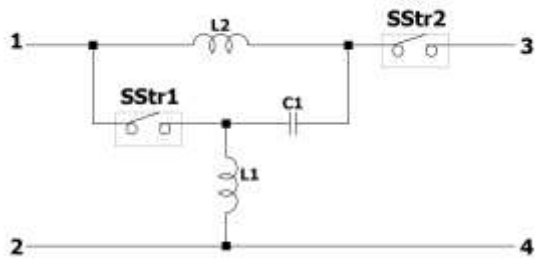

Fig. 1: Basic structure

One switching structure SStr1 or SStr2 is formed by a series connection of two electronic switches S1 and S2 and a diode D1. The other switching structure is formed only by a diode D2. Using a positive input voltage four converters can be designed according to Figure 1. For the second capacitor there are two possibilities for their placement, so one can get eight possible DC/DC converters. When changing the polarity of the input voltage, again eight DC/DC converters originate from Figure 1. Replacing all electronic switches and diodes with current bidirectional switches, two-quadrant DC/DC converters are obtained. The tristate concept changes the voltage transformation ratio of the original converter.

The tristate concept was first applied to the Boost converter, [2], [3], [4]. The application to the Buck-Boost converter can be found in [5]. A very interesting aspect is that with a constant duty cycle of the second switch and controlling the converter by the duty cycle of the first switch, in some cases the converter can be treated as a phase minimum system. The basics of Power Electronics can be studied with the help of the textbooks, e.g. [6], [7], [8]. The modeling and dynamic feedback linearization of a 5-switch tristate Buck-Boost bidirectional DC-DC converter is shown in [9]. A practical applications of a tristate converter is shown in [10], where the tristate converter is used to charge

and discharge supercapacitors in a DC microgrid. It should also be mentioned that the tristate concept can be applied also to converter structures with coupled coils, [11]. The bidirectional non-inverting Buck-Boost converter can also be used as a tristate converter, when both low-side switches are turned on, [12].

2 The Four Basic Structures with a Limited Duty Cycle

The four basic structures are shown in this chapter. They are exemplarily drawn with MOSFETs as electronic switches. The types are numbered by the names that were used in the underlying patent and also in the basic paper [1]. All circuits are shown with C2 between input and output.

2.1 Step-up Converter Type 2b

The converter is depicted in Figure 2. The second capacitor is placed between the input and the output. The input voltage is applied to the connectors 3 and 4. The switch structure SStr1 is realized by a tristate switch combination and the second switch structure is formed only by a diode. The load, here represented by a resistor, is connected between terminals 1 and 2.

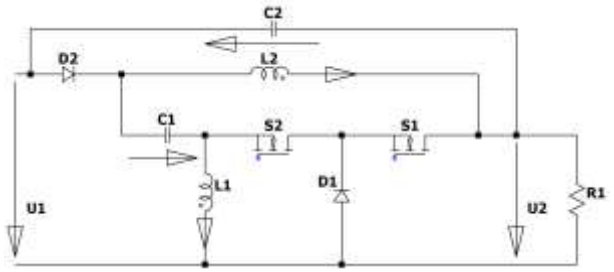

Fig. 2: Tristate step-up converter type 2b with restricted duty cycle

In the steady state, the converter has three modes which follow each other during the switching period. In mode M1 both electronic switches S1 and S2 are on, the output voltage U2, which is equal to the sum of the voltage across C2 and the input voltage U1, is across the coil L1, and the current through it increases. When S1 is turned off, mode M2 begins and the diode D1 turns on and the voltage across L1 is nearly zero and the current stays constant. Mode M3 starts when S2 is turned off, too. Now diode D2 turns on and the voltage across L1 is equal to the sum of the negative voltage across C1 and the input voltage. The voltage across C1 is equal to the output voltage (in the steady state). The voltage-time balance is therefore:

$$U_2 d_1 = \left|U_1 - U_2\right|\left(1 - d_2\right) \tag{1}$$

which leads to the voltage transformation ratio:

$$M = \frac{U_2}{U_1} = \frac{1 - d_2}{1 - d_1 - d_2} \tag{2}$$

with the restrictions:

$$d_1 + d_2 < 1 \text{ and } d_1 \le d_2 \,. \tag{3}$$

The duty cycle of d_2 must be greater or equal to that of the switch S1 d_1. From the voltage transformation ratio, one can see that two possibilities to change the output voltage are feasible. Figure 3 shows the voltage transformation ratio for the variable duty cycle of switch S1 and the duty cycle of switch S2 as a parameter. In Figure 4 the duty cycle of S1 is the parameter and the duty cycle of S2 is the variable.

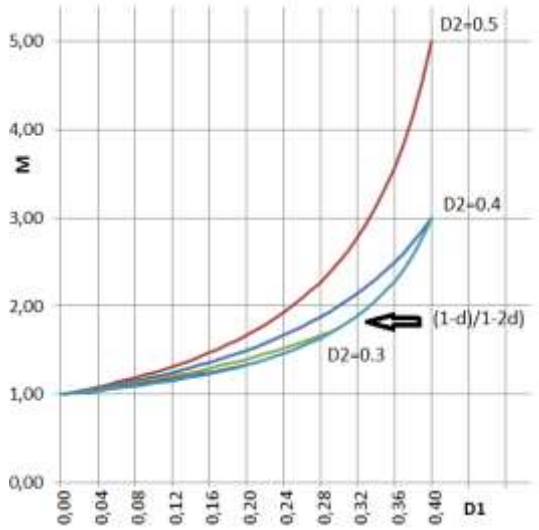

Fig. 3: Voltage transformation ratio of the tristate step-up converter type 2b with d2 as parameter and d1 as variable

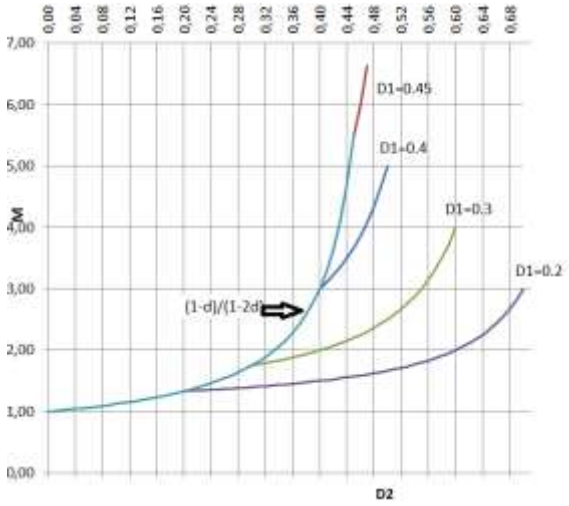

Fig. 4: Voltage transformation ratio of the tristate step-up converter type 2b with d1 as parameter and d2 as variable

The connection between the currents through the coils and the load current is also an important feature of a converter. In the steady-state, the currents through the capacitors are zero in the mean. For the calculation, one can use the mean values of the inductor currents. The current through the first capacitor is the negative current through L2 in modes M1 and M2, and during M3 the positive current through L1. One can write the charge balance according to:

$$\bar{I}_{L2}\, d_2 = \bar{I}_{L1}(1-d_2) \tag{4}$$

During the complete switching period, the capacitor C2 is discharged by the load current. During M1 it is also discharged by the current through L1, and during the off-time of S1 (in the modes M2 and M3) the current through L2 charges the capacitor. The change of charge at the second capacitor must also be zero:

$$-I_{LOAD} - \bar{I}_{L1}\, d_1 + \bar{I}_{L2}(1-d_1) = 0 \tag{5}$$

From (4) and (5) one gets the connections:

$$\frac{\bar{I}_{L1}}{I_{LOAD}} = \frac{d_2}{1-d_1-d_2} \tag{6}$$

$$\frac{\bar{I}_{L2}}{I_{LOAD}} = \frac{1-d_1}{1-d_1-d_2}\,. \tag{7}$$

The steady-state behavior is shown in Figure 5. It shows the voltage across the capacitors, the input current, the currents through the coils, the load current, the output voltage, the input voltage, and the control signals of the switches.

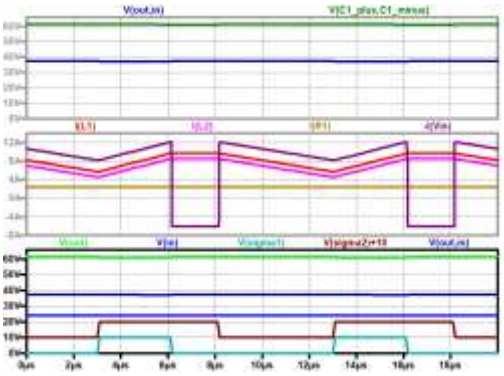

Fig. 5: Tristate step-up converter type_2b with parasitic resistors, up to down: voltage across C1 (dark green), voltage across C2 (dark blue); input current (dark violet), current through L1 (red), current through L2 (violet), load current (brown); output voltage (green), voltage across C2 (dark blue), input voltage (blue), control signal of S2 (black, shifted), control signal of S1 (turquoise).

For this converter type, Figure 6 shows the variant with the second capacitor in parallel to the output and in Figure 7 one can see the important voltages and currents in the steady state.

The input current is pulsating and is only flowing when the switches S1 and S2 are off. The peak of the input current is now also significantly higher.

When a stable input source (batteries or DC microgrid) is used, the variant with the capacitor between input and output is preferable. When the input source is unstable, it is better to use the variant with the capacitor at the output.

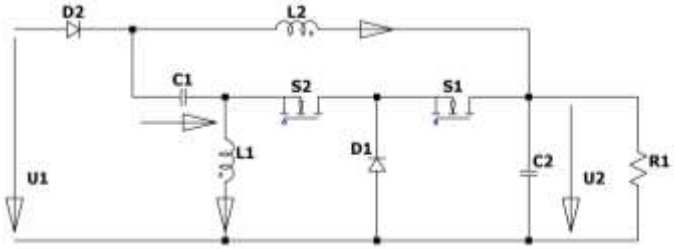

Fig. 6: Tristate step-up converter type 2b, the second capacitor in parallel to the output

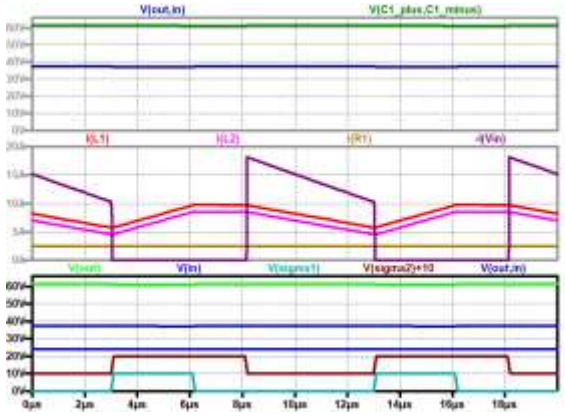

Fig. 7: Tristate step-up converter type 2b and the second capacitor in parallel to the output with parasitic resistors, up to down: voltage across C1 (dark green), voltage across C2 (dark blue); input current (dark violet), current through L1 (red), current through L2 (violet), load current (brown); output voltage (green), voltage across C2 (dark blue), input voltage (blue), control signal of S2 (black, shifted), control signal of S1 (turquoise).

2.2 Step-down Converter Type 2c

The circuit diagram is depicted in Figure 8.

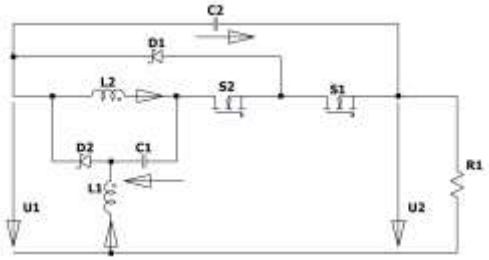

Fig. 8: Tristate step-down converter type 2b with limited duty cycle

The second switching structure is replaced by the tristate switch. The input voltage is connected to the terminals 1 and 2 and the load is connected to the terminals 3 and 4. The first switching structure is the single diode D2.

During mode M1 the voltage across C2 lies across the inductor L2, during M2 the voltage across L2 is zero, and during M3 the voltage across C1 is negative across the coil L2. From the loop U1, L2, C1, and L1 one can see that the voltage across C1 must be equal to the input voltage in a steady state. The voltage across C2 is equal to the difference between the input voltage and the output voltage. The voltage-time balance across L2 can now be written as:

$$(U_1 - U_2)d_1 = |-U_1|(1-d_2) \tag{8}$$

and that leads to the voltage transformation ratio:

$$M = \frac{U_2}{U_1} = \frac{d_1 + d_2 - 1}{d_1} \tag{9}$$

with the limitations:

$$d_1 + d_2 > 1 \text{ and } d_2 \geq d_1 . \tag{10}$$

Figure 9 shows the voltage transformation ratio for the variable duty cycle of switch S1 and the duty cycle for switch S2 as a parameter. In Figure 10 the duty cycle for S1 is the parameter and the duty cycle of S2 is the variable.

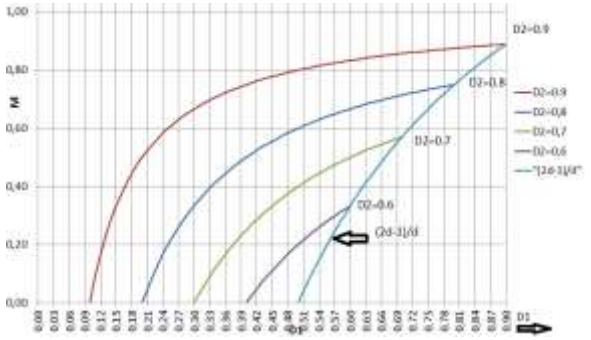

Fig. 9: Voltage transformation ratio of the tristate step-down converter type 2b with d2 as parameter and d1 as variable

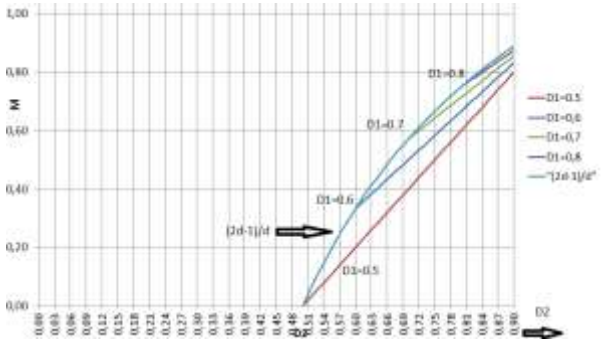

Fig. 10: Voltage transformation ratio of the tristate step-down converter type 2b with d1 as parameter and d2 as variable

The connections between the load current and the mean values of the currents through the coils can be again calculated with the help of the currents through the capacitors. The charge balances for C1 and C2 are:

$$\bar{I}_{L1}\, d_2 = \bar{I}_{L2}(1-d_2) \tag{11}$$

$$(-I_{LOAD} + \bar{I}_{L1} + \bar{I}_{L2})d_1 = \bar{I}_{LOAD}(1-d_2), \tag{12}$$

respectively, and leading to the connections:

$$\frac{\bar{I}_{L10}}{I_{LOAD}} = \frac{1-d_2}{d_1} \tag{13}$$

$$\frac{\bar{I}_{L2}}{I_{LOAD}} = \frac{d_2}{d_1} . \tag{14}$$

Figure 11 shows the input current which is now continuously compared to the variant where the second capacitor is in parallel to the output and where the current is pulsating, furthermore, it shows the currents through the coils, the load current, the input and the output voltages and the control signals. Figure 12 shows the same signals for the variant, where the second capacitor is in parallel to the output.

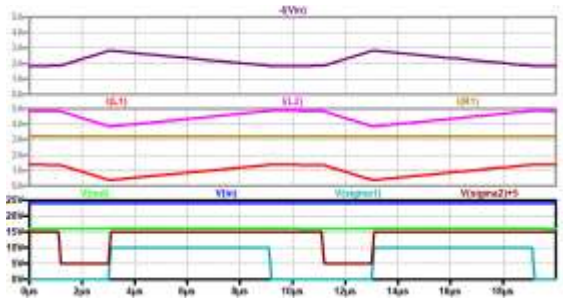

Fig. 11: Tristate step-down converter type 2c with parasitic resistors, up to down: input current (dark violet); current through L2 (violet), load current (brown), current through L1 (red); output voltage (green), control signal of S2 (black, shifted), control signal of S1 (turquoise)

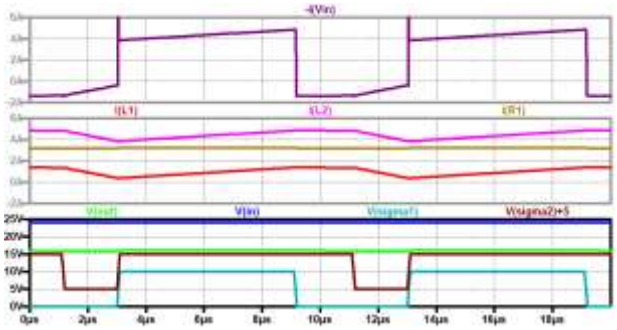

Fig. 12: Tristate step-down converter type 2c second capacitor in parallel to the load with parasitic resistors, up to down: input current (dark violet); current through L2 (violet), load current (brown), current through L1 (red); output voltage (green), control signal of S2 (black, shifted), control signal of S1 (turquoise)

2.3 Step-up-down Converter Type 3d

The input voltage is connected to terminals 3 and 4, the switching structure SStr2 is a tristate switch and SStr1 is now a diode (Figure 13). The second capacitor is connected between the input and the output.

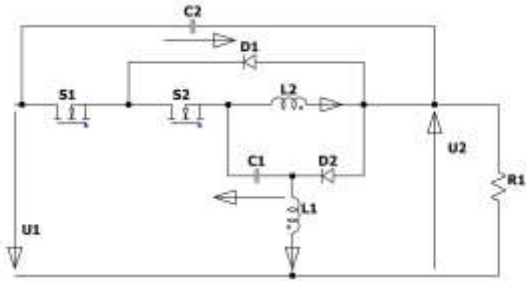

Fig. 13: Tristate step-up-down converter with limited duty cycle type 3d

When both switches are on, the voltage across coil L2 is equal to the voltage across C2 which is equal to the sum of the input and the output voltages. When S1 is turned off, the voltage across L2 is zero and when S2 is also turned off, diode D2 turns on and the voltage across L2 is equal to the negative voltage across C1. It is easy to see that the voltage across C1 is equal to the output voltage in the steady state. The voltage-time balance across L2 is equal to:

$$(U_1 + U_2)d_1 = U_2(1-d_2) \tag{15}$$

leading to the voltage transformation ratio:

$$M = \frac{U_2}{U_1} = \frac{d_1}{1-d_1-d_2} \tag{16}$$

with the limitations:

$$d_1 + d_2 < 1 \text{ and } d_2 \geq d_1 . \tag{17}$$

Figure 14 shows the voltage transformation ratios of the duty cycle of switch S2 as constant and the duty cycle of switch S1 as variable.

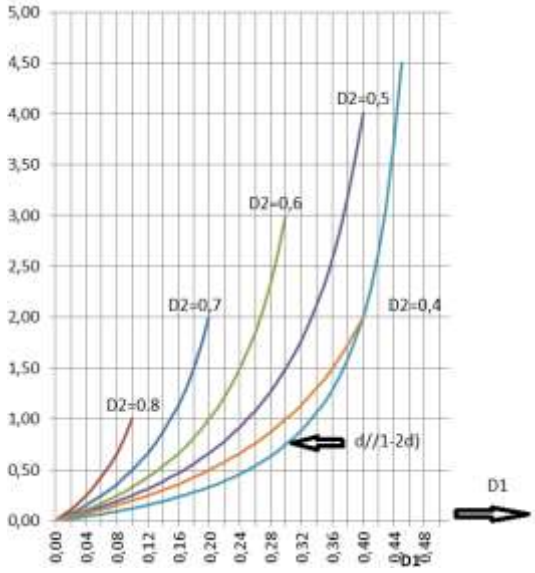

Fig. 14: Voltage transformation ratio of the tristate step-up-down converter type 3d with d2 as parameter and d1 as variable

In Figure 15 the parameter is a constant duty cycle of S1 and the variable is the duty cycle of S2.

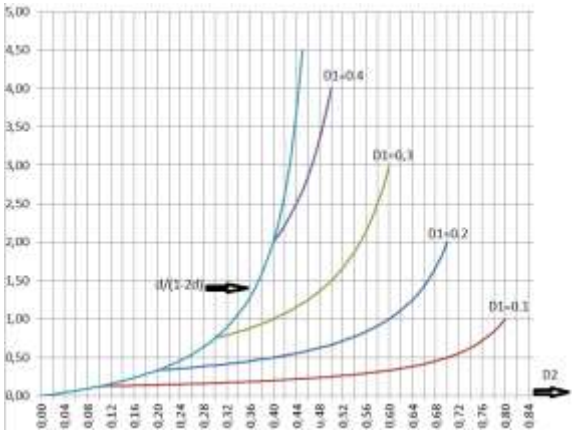

Fig. 15: Voltage transformation ratio of the tristate step-up-down converter type 3d with d1 as parameter and d2 as variable

For the connections between the load current and the mean values of the current through the coils one gets from the charge balances

$$\bar{I}_{L1}\, d_2 = \bar{I}_{L2}(1-d_2) \tag{18}$$

$$(I_{LOAD} + \bar{I}_{L2})d_1 = (\bar{I}_{L1} - I_{LOAD})(1-d_1) \tag{19}$$

$$\frac{\bar{I}_{L1}}{I_{LOAD}} = \frac{1-d_2}{1-d_1-d_2} \tag{20}$$

$$\frac{\bar{I}_{L2}}{I_{LOAD}} = \frac{d_2}{1-d_1-d_2} \quad . \tag{21}$$

Figure 16 shows the signals input current, currents through the coils, input and output voltages, and the control signals of the active switches. One can again see that the input current is continuous when the second capacitor is between the output and the input.

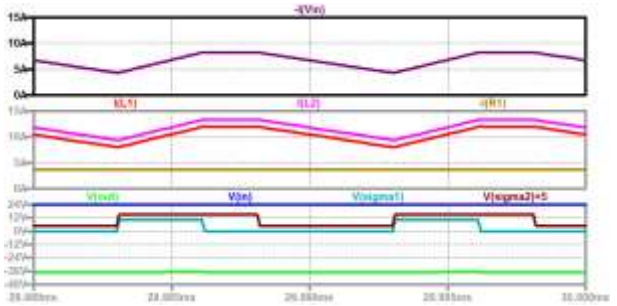

Fig. 16: Tristate step-up-down converter type 3d with parasitic resistors, up to down: input current (dark violet); current through L2 (violet), load current (brown), current through L1 (red); output voltage (green), control signal of S2 (black, shifted), control signal of S1 (turquoise)

2.4 Step-up-down Converter Type 2a

The input voltage is connected to the terminals 1 and 2, the load is connected to the terminals 3 and 4. The second capacitor is placed between the input and the output. The switching structure SStr1 is now the tristate switch and SStr2 is replaced by a diode (Figure 17).

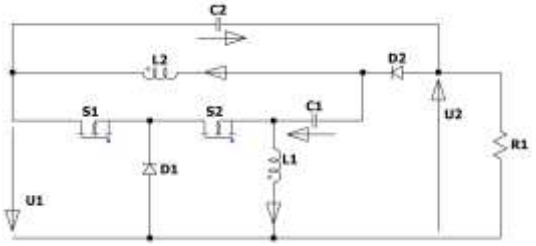

Fig. 17: Tristate step-up-down converter with limited duty cycle type 2a

From the circuit diagram one can obtain for the steady state that the voltage across C1 must be equal to the input voltage and the voltage across C2 must be equal to the sum of the input voltage and the output voltage. During mode M1 (both active switches are on) the input voltage is across the coil L1. During mode M2 (S2 and D1 are on) the coil L1 is short-circuited and the voltage across it is zero. During M3 (only D2 is conducting) the voltage across L1 is the negative sum of the voltage across C1 (which is equal to the input voltage) and the output voltage. The voltage-time balance across L1 is therefore:

$$U_1 d_1 = (U_1 + U_2)(1-d_2) \tag{22}$$

$$M = \frac{U_2}{U_1} = \frac{d_1 + d_2 - 1}{1-d_2} \tag{23}$$

with the limitations:

$$d_1 + d_2 > 1 \text{ and } d_2 \geq d_1 \,. \tag{24}$$

Figure 18 shows the voltage transformation ratios for the duty cycle of switch S2 as constant and the duty cycle of switch S1 as variable.

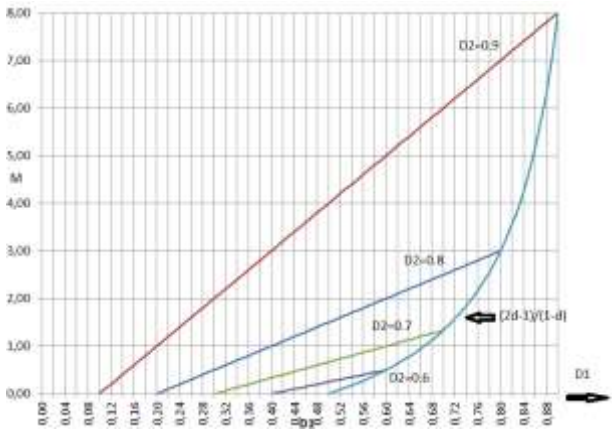

Fig. 18: Voltage transformation ratio of the tristate step-up-down converter type 2a with d2 as parameter and d1 as variable.

In Figure 19 the parameter is a constant duty cycle of S1 and the variable is the duty cycle of S2.

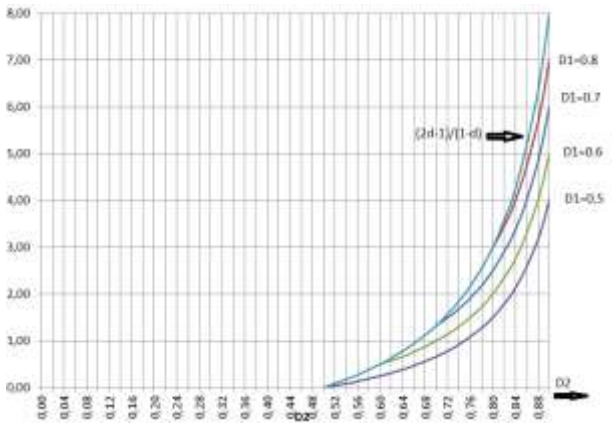

Fig. 19: Voltage transformation ratio of the tristate step-up-down converter type 2a with d2 as parameter and d1 as variable

The charge balance of C1 can be written as:

$$\bar{I}_{L2}\, d_2 = \bar{I}_{L1}(1-d_2) \,. \tag{25}$$

For C2 one gets:

$$I_{LOAD} d_2 = \left(\bar{I}_{L1} + \bar{I}_{L2} - I_{LOAD} \right) (1 - d_2) \qquad (26)$$

leading to:

$$\frac{\bar{I}_{L10}}{I_{LOAD}} = \frac{d_2}{1 - d_2} \qquad (27)$$

$$\frac{\bar{I}_{L2}}{I_{LOAD}} = 1 \ . \qquad (28)$$

The steady-state behavior is shown in Figure 20. The signals are input current, currents through the coils, input and output voltages, and the control signals.

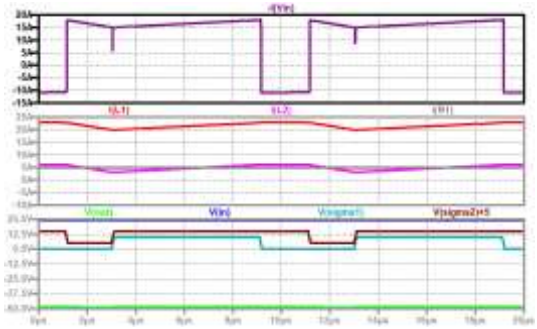

Fig. 20: Tristate step-up-down converter type 2a with parasitic resistors, up to down: input current (dark violet); current through L2 (violet), load current (brown), current through L1 (red); output voltage (green), control signal of S2 (black, shifted), control signal of S1 (turquoise)

The input current is pulsating and when only switch S2 is on current is fed back to the source. Compared to the variant with the second capacitor parallel to the load the peak current is reduced and the time during which the current is fed back to the source is shorter. This is shown in Figure 21. If one wants to avoid reverse current into the source it is better to use the topology according to type 3d.

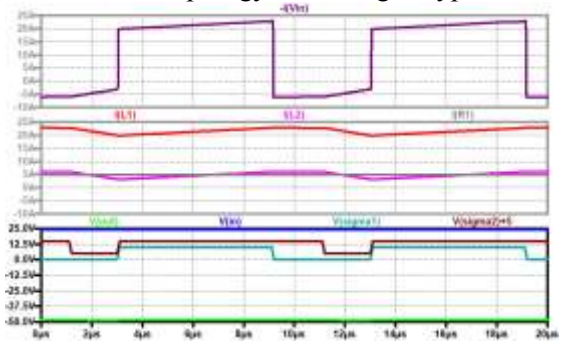

Fig. 21: Tristate step-up-down converter type 2a, C2 in parallel to the output, with parasitic resistors, up to down: input current (dark violet); current through L2 (violet), load current (brown), current through L1 (red); output voltage (green), control signal of S2 (black, shifted), control signal of S1 (turquoise)

3 Topologies of the Four Converters Supplied by a Negative Input Voltage

To construct converters for a negative input voltage one has to change the polarity of the semiconductors. Again only the converters with the second capacitor between input and output are shown. The number of the topologies correlates with [1]. The results are the same as for the corresponding ones in paragraph 2. Figure 22 shows the step-up converter for negative input voltage. Figure 23 is the step-up converter, Figure 24 is the step-down converter, and Figure 25 is the second possible step-up-down converter for negative input voltage.

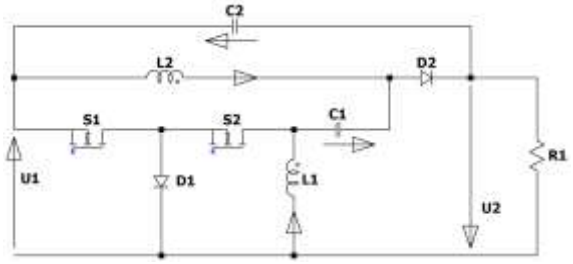

Fig. 22: Tristate step-up-down converter type 3a

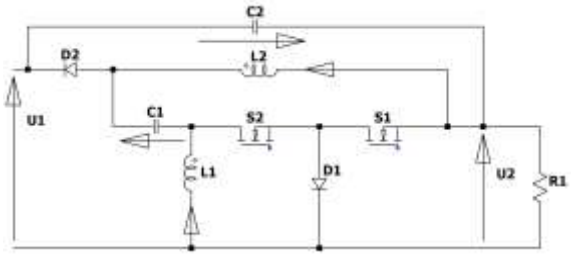

Fig. 23: Tristate step-up converter type 3b

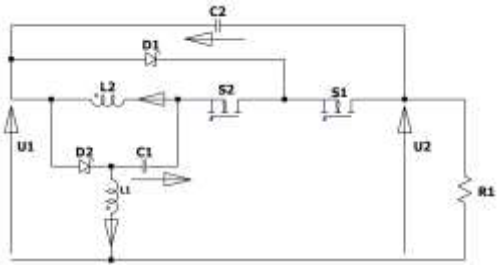

Fig. 24: Tristate step- down converter type 3c

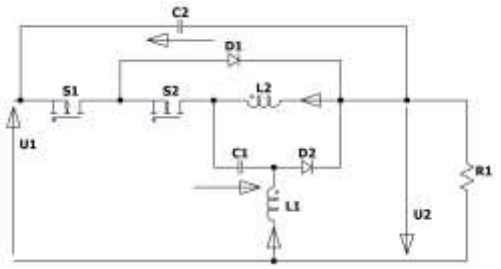

Fig. 25: Tristate step-up-down converter type 2d

4 Further Interesting Aspects

The voltages across the coils are equal to each other, therefore one can combine the two coils on one magnetic core (integrated magnetics). One can also combine two converters in parallel to increase the power. In this case, the control signals for the second converter should be shifted by a half period. When more than two converters work together, the signals should be shifted by 120 degrees for three converters or by 90 degrees, when four converters are working together. For increasing the voltage transformation ratio two (or more) converters can be cascaded.

4.1 Model of the Converter Type 2b

The model of the converter for ideal components is derived for the continuous mode. The equivalent circuit for mode M1 (both active switches are on) is depicted in Figure 26.

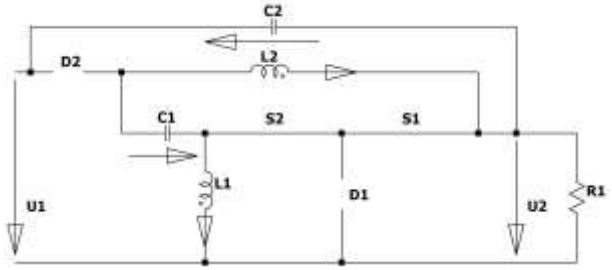

Fig. 26: Equivalent circuit mode M1

The state equations are given by

$$\frac{di_{L1}}{dt} = \frac{u_{C2} + u_1}{L_1} \tag{29}$$

$$\frac{di_{L2}}{dt} = \frac{u_{C1}}{L_2} \tag{30}$$

$$\frac{du_{C1}}{dt} = -\frac{i_{L2}}{C_1} \tag{31}$$

$$\frac{du_{C2}}{dt} = -\frac{i_{L1} + (u_{C2} + u_1)/R_1}{C_2} . \tag{32}$$

For mode M2 (S2 is still on and D1 is conducting) the equivalent circuit is shown in Figure 27.

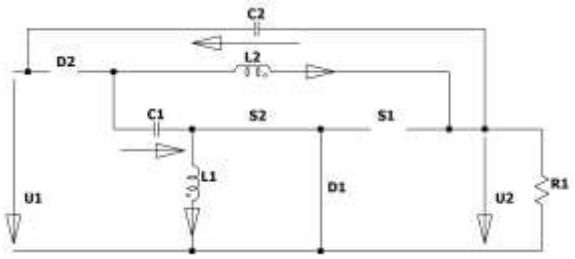

Fig. 27: Equivalent circuit mode M2

The state equations are now given by:

$$\frac{di_{L1}}{dt} = \frac{"0"}{L_1} \tag{33}$$

$$\frac{di_{L2}}{dt} = \frac{u_{C1} - (u_{C2} + u_1)}{L_2} \tag{34}$$

$$\frac{du_{C1}}{dt} = -\frac{i_{L2}}{C_1} \tag{35}$$

$$\frac{du_{C2}}{dt} = \frac{i_{L2} - (u_{C2} + u_1)/R_1}{C_2} . \tag{36}$$

The equivalent circuit of mode M3 (only diode D2 is conducting) can be seen in Figure 28.

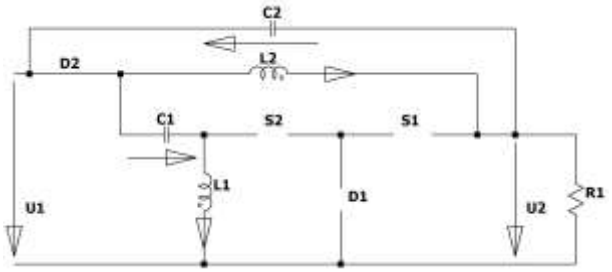

Fig. 28: Equivalent circuit mode M3

$$\frac{di_{L1}}{dt} = \frac{-u_{C1} + u_1}{L_1} \tag{37}$$

$$\frac{di_{L2}}{dt} = -\frac{u_{C2}}{L_2} \tag{38}$$

$$\frac{du_{C1}}{dt} = \frac{i_{L1}}{C_1} \tag{39}$$

$$\frac{du_{C2}}{dt} = \frac{i_{L2} - (u_{C2} + u_1)/R_1}{C_2} . \tag{40}$$

The three sets of equations can be combined into one describing matrix differential equation. This is possible when the switching period of the converter is much shorter than the time constants of the converter. The equations are weighted by the duty cycles (the time at which they are valid divided by the switching period). Mode M1 is weighted by d_1, mode M2 is weighted by (d_2-d_1), and M3 is weighted by $(1-d_2)$. This leads to:

$$\frac{d}{dt}\begin{pmatrix} i_{L1} \\ i_{L2} \\ u_{C1} \\ u_{C2} \end{pmatrix} = \begin{bmatrix} 0 & 0 & \frac{d_2-1}{L_1} & \frac{d_1}{L_1} \\ 0 & 0 & \frac{d_2}{L_2} & \frac{d_1-1}{L_2} \\ \frac{1-d_2}{C_1} & -\frac{d_2}{C_1} & 0 & 0 \\ -\frac{d_1}{C_2} & \frac{1-d_1}{C_2} & 0 & -\frac{1}{R_1 C_2} \end{bmatrix} \begin{pmatrix} i_{L1} \\ i_{L2} \\ u_{C1} \\ u_{C2} \end{pmatrix} + \begin{bmatrix} \frac{1+d_1-d_2}{L_1} \\ \frac{d_1-d_2}{L_2} \\ 0 \\ -\frac{1}{R_1 C_2} \end{bmatrix} (u_1) \quad . \quad (41)$$

From this equation, one can get the operation point connections and the small signal model. (41) is a nonlinear differential equation. To get transfer functions and Bode plots which are very helpful for the controller design, one has to linearize the equation around the working point. The variables are substituted by the sum of the working point value, written with capital letters and a zero in the index, and the disturbance, written with small letters and a roof on top. The working point connections result in the voltages in:

$$(D_{20}-1)U_{C10} + D_{10}U_{C20} + (1+D_{10}-D_{20})U_{10} = 0 \quad (42)$$

$$D_{20}U_{C10} + (D_{10}-1)U_{C20} + (D_{10}-D_{20})U_{10} = 0 \, . \quad (43)$$

For the current one obtains:

$$(1-D_{20})I_{L10} - D_{20}I_{L20} = 0 \quad (44)$$

$$-D_{10}I_{L10} + (1-D_{10})I_{L20} - \frac{U_{C20}}{R_1} - \frac{U_{10}}{R_1} = 0 \, . \quad (45)$$

For the connections of the capacitor voltages and the output voltage referred to as the input voltage one gets:

$$\frac{U_{C10}}{U_1} = \frac{1-D_{20}}{1-D_{10}-D_{20}} \, , \quad (46)$$

$$\frac{U_{C20}}{U_1} = \frac{D_{10}}{1-D_{10}-D_{20}} \, , \quad (47)$$

$$\frac{U_{20}}{U_1} = \frac{D_{10}}{1-D_{10}-D_{20}} + 1 = \frac{1-D_{20}}{1-D_{10}-D_{20}} \, , \quad (48)$$

respectively.

These results are equal to the results which were obtained with the help of inspection, as shown in paragraph 2.1.

From (41) one can also find the small signal model of the converter around the working point. The real values are found by adding the result of the small signals with the operating point values. The small signal model can be written according to:

$$\frac{d}{dt}\begin{pmatrix} \hat{i}_{L1} \\ \hat{i}_{L2} \\ \hat{u}_{C1} \\ \hat{u}_{C2} \end{pmatrix} = \begin{bmatrix} 0 & 0 & \frac{D_{20}-1}{L_1} & \frac{D_{10}}{L_1} \\ 0 & 0 & \frac{D_{20}}{L_2} & \frac{D_{10}-1}{L_2} \\ \frac{1-D_{20}}{C_1} & -\frac{D_{20}}{C_1} & 0 & 0 \\ -\frac{D_{10}}{C_2} & \frac{1-D_{10}}{C_2} & 0 & -\frac{1}{R_1 C_2} \end{bmatrix} \begin{pmatrix} \hat{i}_{L1} \\ \hat{i}_{L2} \\ \hat{u}_{C1} \\ \hat{u}_{C2} \end{pmatrix} + \begin{bmatrix} \frac{1+D_{10}-D_{20}}{L_1} & \frac{U_{C20}+U_{10}}{L_1} & \frac{U_{C10}-U_{10}}{L_1} \\ \frac{D_{10}-D_{20}}{L_2} & \frac{U_{C20}+U_{10}}{L_2} & \frac{U_{C10}-U_{10}}{L_2} \\ 0 & 0 & -\frac{I_{L10}+I_{L20}}{C_1} \\ -\frac{1}{R_1 C_2} & -\frac{I_{L10}+I_{L20}}{C_1} & 0 \end{bmatrix} \begin{pmatrix} \hat{u}_1 \\ \hat{d}_1 \\ \hat{d}_2 \end{pmatrix} \quad (49)$$

Using abbreviations for the elements of the state matrix and the input matrix:

$$\frac{d}{dt}\begin{pmatrix} \hat{i}_{L1} \\ \hat{i}_{L2} \\ \hat{u}_{C1} \\ \hat{u}_{C2} \end{pmatrix} = \begin{bmatrix} 0 & 0 & A_{13} & A_{14} \\ 0 & 0 & A_{23} & A_{24} \\ A_{31} & A_{32} & 0 & 0 \\ A_{41} & A_{42} & 0 & A_{44} \end{bmatrix} \begin{pmatrix} \hat{i}_{L1} \\ \hat{i}_{L2} \\ \hat{u}_{C1} \\ \hat{u}_{C2} \end{pmatrix} + \begin{bmatrix} B_{11} & B_{12} & B_{13} \\ B_{21} & B_{22} & B_{23} \\ 0 & 0 & B_{33} \\ B_{41} & B_{42} & 0 \end{bmatrix} \begin{pmatrix} \hat{u}_1 \\ \hat{d}_1 \\ \hat{d}_2 \end{pmatrix} \quad (50)$$

and using the Laplace transformation:

$$\begin{bmatrix} s & 0 & -A_{13} & -A_{14} \\ 0 & s & -A_{23} & -A_{24} \\ -A_{31} & -A_{32} & s & 0 \\ -A_{41} & -A_{42} & 0 & s-A_{44} \end{bmatrix} \begin{pmatrix} I_{L1}(s) \\ I_{L2}(s) \\ U_{C1}(s) \\ U_{C2}(s) \end{pmatrix} = \begin{bmatrix} B_{11} & B_{12} & B_{13} \\ B_{21} & B_{22} & B_{23} \\ 0 & 0 & B_{33} \\ B_{41} & B_{42} & 0 \end{bmatrix} \begin{pmatrix} U_1(s) \\ D_1(s) \\ D_2(s) \end{pmatrix} \quad (51)$$

one can calculate twelve transfer functions between the four state variables and the three input variables. The most important transfer functions are those that show the influence on the voltage across the second capacitor and the duty cycles. The denominator is the same for all twelve transfer functions and can be calculated by the determinant of the coefficient matrix and leads to:

$$Den = s^4 + s^3(-A_{44}) + s^2\begin{pmatrix} -A_{14}A_{41} - A_{24}A_{42} - A_{13}A_{31} \\ -A_{23}A_{32} \end{pmatrix} +$$
$$s(A_{13}A_{31}A_{44} + A_{23}A_{32}A_{44}) + A_{41}(-A_{13}A_{24}A_{32} + A_{14}A_{23}A_{32})$$
$$-A_{42}(-A_{13}A_{24}A_{31} + A_{14}A_{23}A_{31}). \quad (52)$$

The numerator of the transfer function between the voltage across C2 and the duty cycle D1 can be calculated with the method of Crammer to:

$$NUM\_UC1D = B_{42}s^3 + s^2(A_{41}B_{12} + A_{42}B_{22}) +$$
$$s(-A_{13}A_{31}B_{42} - A_{23}A_{32}B_{42}) + \quad (53)$$
$$A_{41}(A_{13}A_{32}B_{22} - A_{23}A_{32}B_{12}) - A_{42}(A_{13}A_{31}B_{22} - A_{23}A_{31}B_{12})$$

With the same method, the numerator for the transfer function between the voltage across C2 and the duty cycle of the second switch D2 can be calculated and leads to:

$$NUM\_UC2D2 = s^2(A_{41}B_{13} + A_{42}B_{23}) + s\begin{pmatrix} A_{13}A_{41}B_{33} \\ +A_{23}A_{42}B_{33} \end{pmatrix} +$$
$$+A_{41}(A_{13}A_{32}B_{23} - A_{23}A_{32}B_{13}) - A_{42}\begin{pmatrix} A_{13}A_{31}B_{23} - \\ A_{23}A_{31}B_{13} \end{pmatrix}. \quad (54)$$

The parameters used in all simulations are L1=L2=47µH, C1=C2=330µF, and U1=24 V, (the parasitic resistors are 4 mΩ for the coils and 10 mΩ for the capacitors). The working point for the calculation of the Bode plot is D10=0.3, D20=0.5, UC10=60 V, UC20=36 V, ILOAD=2.4 A, IL10=8.4 A, IL20=6 A, R=25 Ω.

Figure 29 shows the Bode plot of the voltage across C2 in dependence on the duty cycle d1. The transfer function is a non-phase minimum system because one zero is on the right side of the complex plane. The complex zero leads to a resonance at 904 Hz and is on the left side of the complex plane and shifts the phase to +180°, the third zero is on the right side and shifts the phase tending to -90°. The complex poles are at 507 Hz and at 1228 Hz and can be seen as the two positive spikes. On the whole the phase tends now only to -270°.

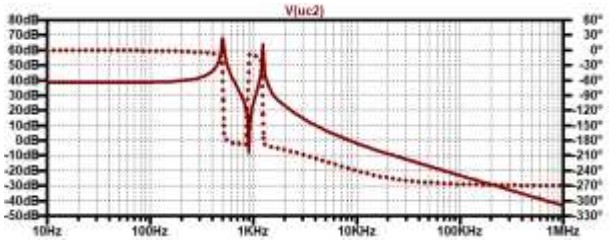

Fig. 29: Bode plot voltage across C2 in dependence on D1 (solid line: gain response, dotted line: phase response)

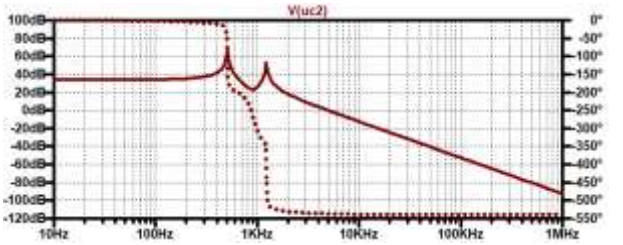

Fig. 30: Bode plot voltage across C2 in dependence on D2 (solid line: gain response, dotted line: phase response)

Figure 30 shows the Bode plot for the voltage across C2 in dependence on the duty cycle of switch S2. The transfer function of the voltage across C2 and D2 is a non-phase minimum system. The complex zero is on the right half of the complex plane and shifts the phase by a further minus 180°. So the phase tends to be minus 540°.

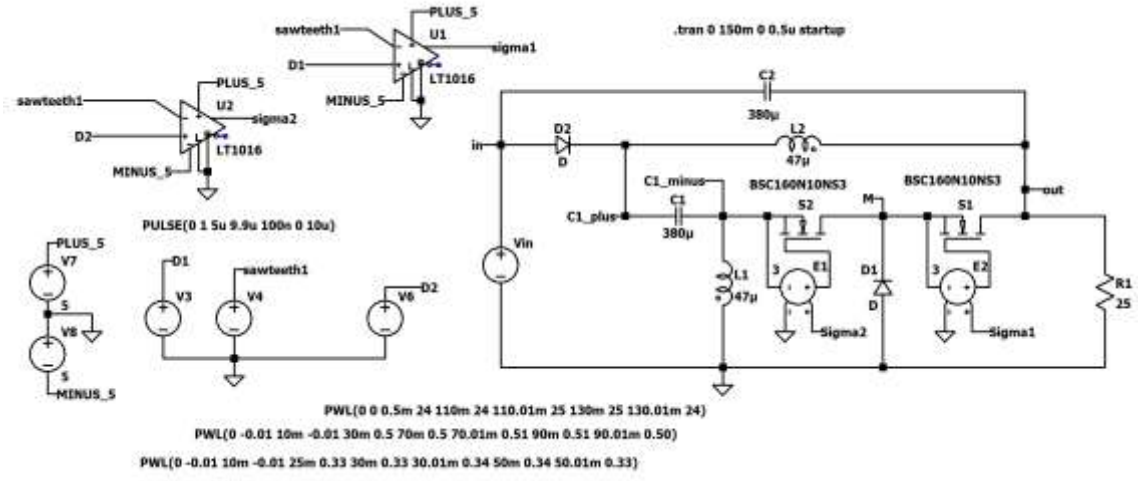

Fig. 31: Simulation circuit

Figure 31 shows the LTSpice simulation circuit with parasitic resistors included in the models of the coils and the capacitors. The pulse width modulation is generated with the help of the comparators U1 and U2. The voltage sources V3 and V6 produce the duty cycles which are compared with the saw tooth signal of V4. The comparators must be supplied by plus and minus 5 V. Therefore, the drivers E1 and E2 which control the MOSFETs must amplify the control signals. The isolated drivers are modeled by voltage-controlled voltage sources.

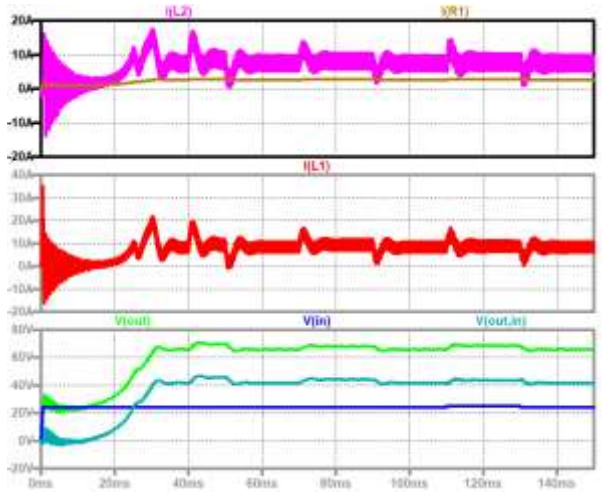

Fig. 32: Current through L2 (violet), load current (brown); current through L1 (red); output voltage (green), voltage across C2 (turquoise), input voltage (blue).

Figure 32 and Figure 33 show the results.

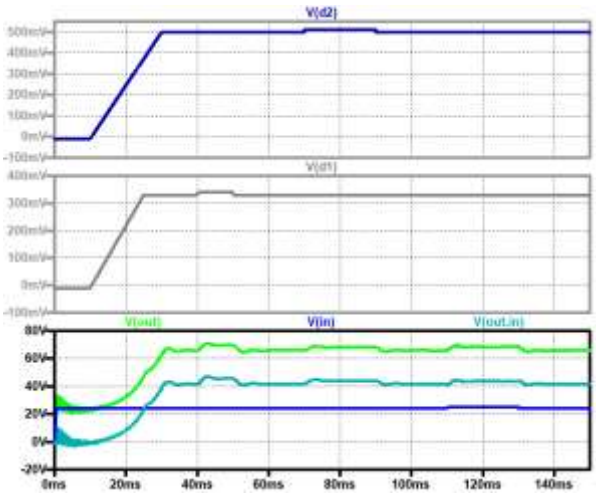

Fig. 33: Up to down: duty cycle for switch S2 (dark blue); duty cycle for switch S1 (grey); output voltage (green), voltage across C2 (turquoise), input voltage (blue)

The input voltage is a stable voltage that is turned on within 0.5 ms. In this case, there is a short inrush peak and some damped ringing. After 10 ms a soft-start begins and the duty cycles for the two electronic switches increase linearly in the next 20 ms. The duty cycle for S1 makes a step at 40 ms up and down at 50 ms. At 70 ms the duty cycle of S2 makes a step up and returns to the original value 20 ms later. At 110 ms the input voltage makes a step up and returns after 20 ms. The lowest graph shows the output voltage, the voltage across C2, and the input voltage. Each step shows a damped ringing as a reaction. The currents through the coils show a more pronounced transient.

5 Conclusion

Starting from the structure Figure 1, four new converters were generated and described. When the input voltage is negative, again four new converters can be designed and the circuits are shown. The function is the same as for the converters with positive input voltage. The new converters can be connected in parallel and controlled in an interleaved way to improve the input current. Two possible positions of C2 lead to eight new converters. Using bidirectional switches instead of the active and the passive switches leads to bidirectional converters and generates 16 additional DC/DC converters.

The converters have several interesting features:

- Additional degree of freedom in the voltage transformation ratio
- Limited duty cycle
- Interesting voltage transformation ratios
- Possibility to couple and combine the coils on one magnetic core
- Input current is influenced depending on the position of the second capacitor.
-

The converters can be applied for solar and DC microgrids and other applications.

References:

[1] F. A. Himmelstoss, and M. Jungmayer, A Family of Modified Converters with Limited Duty Cycle, 2021 *International Aegean Conference on Electrical Machines and Power Electronics (ACEMP) & 2021 International Conference on Optimization of Electrical and Electronic Equipment (OPTIM)*, Brasov, Romania, 2021, pp. 246-253.

[2] K. Viswanathan, R. Oruganti and D. Srinivasan, Dual-mode control of tri-state

boost converter for improved performance, *IEEE Transactions on Power Electronics*, vol. 20, no. 4, pp. 790-797, July 2005, doi: 10.1109/TPEL.2005.850907.

[3] K. Viswanathan, R. Oruganti and D. Srinivasan, A novel tri-state boost converter with fast dynamics, *IEEE Transactions on Power Electronics*, vol. 17, no. 5, pp. 677-683, Sept. 2002, doi: 10.1109/TPEL.2002.802197.

[4] S. K. Viswanathan, R. Oruganti and D. Srinivasan, Dual mode control of tri-state boost converter for improved performance, *IEEE 34th Annual Conference on Power Electronics Specialist*, Acapulco, Mexico, 2003, pp. 944-950 vol.2, doi: 10.1109/PESC.2003.1218182.

[5] N. Rana and S. Banerjee, Interleaved Tri-state Buck-Boost Converter with Fast Transient Response and Lower Ripple, *2019 IEEE Transportation Electrification Conference (ITEC-India)*, Bengaluru, India, 2019, pp. 1-5.

[6] N. Mohan, T. Undeland and W. Robbins, *Power Electronics, Converters, Applications and Design*, 3rd ed. New York: W. P. John Wiley & Sons, 2003.

[7] F. Zach, *Power Electronics*, in German: Leistungselektronik, Frankfurt: Springer, 6th ed., 2022.

[8] Y. Rozanov, S. Ryvkin, E. Chaplygin, P. Voronin, *Power Electronics Basics*, CRC Press, 2016.

[9] G. R. Broday, G. Damm, W. Pasillas-Lépine and L. A. C. Lopes, Modeling and dynamic feedback linearization of a 5-switch tri-state buck-boost bidirectional DC-DC converter, *2021 22nd IEEE International Conference on Industrial Technology (ICIT)*, Valencia, Spain, 2021, pp. 427-432, doi: 10.1109/ICIT46573.2021.9453569.

[10] A. Choubey and L. A. C. Lopes, A tri-state 4-switch bi-directional converter for interfacing supercapacitors to DC micro-grids, *2017 IEEE 8th International Symposium on Power Electronics for Distributed Generation Systems (PEDG)*, Florianopolis, Brazil, 2017, pp. 1-6, doi: 10.1109/PEDG.2017.7972507.

[11] M. A. Vaghela and M. A. Mulla, Tri-State Coupled Inductor Based High Step-Up Gain Converter Without Right Hand Plane Zero, in *IEEE Transactions on Circuits and Systems II: Express Briefs*, vol. 70, no. 6, pp. 2291-2295, June 2023, doi: 10.1109/TCSII.2023.3237679.

[12] Q. Wang, A. Choubey and L. A. C. Lopes, "Mode Transition for Increased Voltage Gain Range of a 4-Switch DC-DC Converter with Tri-State and Single Duty Cycle Control," *2021 IEEE 12th International Symposium on Power Electronics for Distributed Generation Systems (PEDG)*, Chicago, IL, USA, 2021, pp. 1-6, doi: 10.1109/PEDG51384.2021.9494256.

Contribution of Individual Authors to the Creation of a Scientific Article (Ghostwriting Policy)

The author contributed to the present research, in all stages from the formulation of the problem to the final findings and solution.

Sources of Funding for Research Presented in a Scientific Article or Scientific Article Itself

No funding was received for conducting this study.

Conflict of Interest

The author has no conflicts of interest to declare.

Creative Commons Attribution License 4.0 (Attribution 4.0 International, CC BY 4.0)

This article is published under the terms of the Creative Commons Attribution License 4.0
https://creativecommons.org/licenses/by/4.0/deed.en_US